High (1 GHz) repetition rate compact femtosecond laser: A powerful multiphoton tool for nanomedicine and nanobiotechnology

A. Ehlers[a] and I. Riemann
Fraunhofer Institute of Biomedical Technology (IBMT), Ensheimer Strasse 48, D-66386 St. Ingbert, Germany

S. Martin
JenLab GmbH, Schillerstrasse 1, D-07745 Jena, Germany

R. Le Harzic
Fraunhofer Institute of Biomedical Technology (IBMT), Ensheimer Strasse 48, D-66386 St. Ingbert, Germany

A. Bartels and C. Janke
Gigaoptics GmbH, Blarerstrasse 56, D-78462 Konstanz, Germany

K. König
Fraunhofer Institute of Biomedical Technology (IBMT), Ensheimer Strasse 48, D-66386 St. Ingbert, Germany and Faculty of Mechatronics, Saarland University, Postfach 151150, D-66041 Saarbrücken, Germany

Multiphoton tomography of human skin and nanosurgery of human chromosomes have been performed with a 1 GHz repetition rate laser by the use of the commercially available femtosecond multiphoton laser tomograph DermaInspect as well as a compact galvoscanning microscope. We performed the autofluorescence tomography up to 100 μm in the depth of human skin. Submicron cutting lines and hole drillings have been conducted on labeled human chromosomes. © *2007 American Institute of Physics.* [DOI: 10.1063/1.2745367]

I. INTRODUCTION

As the development of laser sources progresses, their possible applications for biomedical applications have to be evaluated. Due to the optical window in the near-infrared (NIR) region, femtosecond Ti:sapphire lasers are the ideal sources for *in vitro* and *in vivo* multiphoton microscopies of biological tissue. Multiphoton autofluorescence imaging of endogenous fluorophores inside the human tissue with NIR femtosecond lasers for the diagnosis of skin is an established method.[1–6] It permits a painless examination of patients without the necessity to introduce narcotics and fluorescent dyes. Photons absorbed via multiphoton excitation can induce autofluorescence based on naturally occurring endogenous fluorescent biomolecules such as flavines, reduced nicotinamide adenine dinucleotide(phosphate) [NAD(P)H], coenzymes, metal-free porphyrins, components of lipofuscin, melanin, elastin, and keratin.[4] Second harmonic generation (SHG) of collagen is a further process that provides an accessible information.[7]

Conventional laser sources used for multiphoton microscopy have typical repetition rates in the megahertz range with pulse lengths of 70–170 fs. It was shown by Chu *et al.*[8] that Ti:sapphire lasers with repetition rates in the gigahertz regime are promising tools for imaging applications. In contrast to conventionally used femtosecond lasers in the NIR, gigahertz lasers offer the advantage of higher number of pulses while keeping the peak intensity at the same level.

This provides a higher signal intensity without increasing photodamage. Furthermore, it allows reducing the peak intensity and by that possible damaging effects while conserving the ability to produce high-resolution multiphoton imaging without staining.

As well, near-infrared femtosecond laser pulses are tools for ultraprecise intracellular and intratissue surgery, cell isolation, and nanostructuring of biomaterials.[9–14] The required high transient laser intensity of TW/cm^2 for multiphoton ablation can be achieved with low nanojoule energy laser pulses when using focusing optics of high numerical aperture.

In this work we performed experiments with a 1 GHz repetition rate laser for multiphoton tomography of human skin by the use of a commercially available femtosecond multiphoton laser tomograph and for nanosurgery of chromosomes.

II. MATERIALS AND METHODS

A. Instrumentation

We used a compact ($18 \times 40 \times 10$ cm^3) Ti:sapphire femtosecond laser oscillator with a high repetition rate of 1 GHz with a continuous tuning range from 750 to 850 nm of the central wavelength[15,16] (GigaJet 20c, prototype version Gigaoptics GmbH, Germany). The oscillator delivers pulses of about 60 fs at an average power of 650 mW (measured as described below). For this study, we used a fixed wavelength of 750 nm.

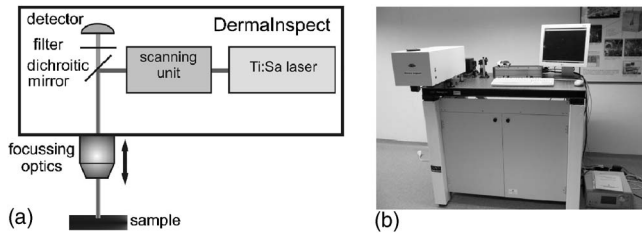a)Electronic mail: alexander.ehlers@ibmt.fraunhofer.de

FIG. 1. Scheme and image of the DermaInspect system with the Gigajet 20c laser. The laser beam is introduced in a galvoscanning unit, expanded, and deflected into a piezodriven high numerical aperture focusing optics.

The laser was coupled into two different imaging systems: (i) a multiphoton tomograph (DermaInspect, JenLab GmbH, Germany) for skin imaging and (ii) a galvoscanning microscope (FemtoCut, JenLabGmbH, Germany) for imaging and nanoprocessing. The DermaInspect system is a clinically approved multiphoton autofluorescence tomograph. It is described in detail elsewhere.[4] Key features relevant to this work are (see Fig. 1) a galvoscanning unit (GSI Lumonics, Inc., USA), a piezodriven (Piezosystems Jena GmbH, Germany) $40\times$ focusing optics with numerical aperture (NA) 1.3 and a photomultiplier tube (PMT) (H5773P, Hamamatsu Photonics K.K., Japan). The system was further equipped with a 700 nm shortpass filter (AHF Analysentechnik AG, Germany) to prevent scattered or reflected laser light onto the detector. Mean laser powers were measured with a standard power meter (FieldMate, Coherent Inc. USA, with PM3 sensor head, maximum power of 2 W); the focusing optics of the tomograph as well as the objective of the scanning microscope were used without oil for pulse power measurements. A maximum power output of 88 mW after transmission through the tomograph could be realized with this laser source corresponding to a pulse energy of 0.09 nJ. Scheme and photograph of the galvoscanning microscope are depicted in Fig. 2. The instrument is based on a standard inverted fluorescence microscope (Zeiss Axiovert, Carl Zeiss AG, Germany) with a laser-scanning module designed for femtosecond laser manipulation (JenLab GmbH, Germany) attached to the side port. A $100\times$ (oil) focusing objective with a numerical aperture of 1.3 (Carl Zeiss AG, Germany) has been employed. A maximum average power output of 130 mW with the gigahertz laser source was achieved.

B. Samples and imaging conditions

Green-fluorescent nanobeads with a diameter of 0.2 μm adhering to a cover slide were used to determine the point spread function[17] (PSF) and for general alignment, 6 μm fluorescent microbeads (both Polysciences, Inc., USA) were employed. All pulse widths were determined with the autocorrelator "MINI" (APE GmbH, Germany), which features an external semiconductor diode for measurement of the laser pulse width in the focus of the high NA optics after passing through the laser systems As biological samples, an *Elodea densa* plant tissue consisting of two cell layers and an excised human skin from frozen storage were employed. Studies on the healthy human skin were carried out on the left forearm of a female volunteer. All samples were imaged with multiple scan rates between 4.4 and 13.4 s/frame. Hu-
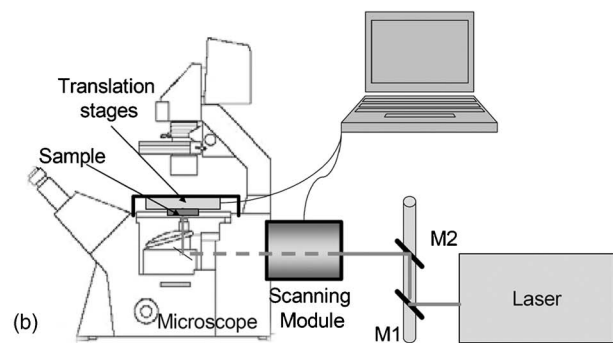
FIG. 2. Schematic diagram and photograph of the galvoscanning microscope used for nanoprocessing.

man metaphase chromosomes prepared from peripheral blood by standard methods[18,19] were placed into a sterile cell chamber (MiniCeM, JenLab GmbH, Germany) and left to dry. One group of chromosomes was labeled with a 5% Giemsa (Merck KGaA, Germany) solution. All chromosome samples were laser processed with the laser-scanning microscope by single line scans and single point illumination at a scan rate of 17 ms/line (512 pixels, corresponding to 20 μm). The processing parameters resulted in a beam dwell time of 51 μs/pixel, thus 51 μs $\times$ 1 GHz $\approx$ 51 000 pulses with a peak power of 0.4 kW. Per single point, the chromosomes were exposed to an accumulated light energy of 0.1 nJ $\times$ 51 000 pulses=5 μJ. For analysis of the laser processed chromosomes, we employed an atomic force microscope (Topometrix, Santa Clara, USA). The samples were investigated in contact mode with 8 lines/s, creating a 512 $\times$ 512 pixel image with a physical size of 16×16 μm^2.

C. Data analysis

The contrast and signal-to noise ratio (SNR) were calculated by comparing the medium intensities of two 100 $\times$ 100 pixel sections of an image showing fluorescent structures (yielding I_{max}) and background areas (yielding I_{min}), respectively,

$$\text{contrast} = \frac{I_{max} - I_{min}}{I_{max} + I_{min}}, \tag{1}$$
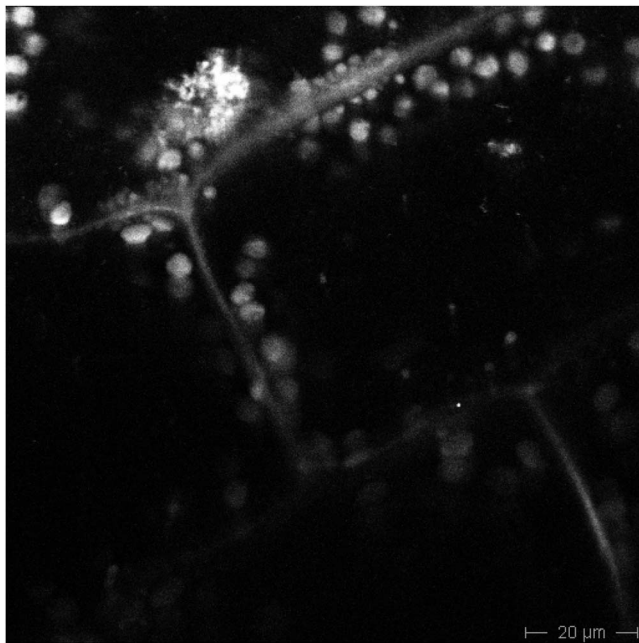
FIG. 3. Two-photon autofluorescence image of *Elodea* leaf. No instantaneous photodamage was detectable.

$$\text{SNR} = \frac{I_{\max}}{I_{\min}}. \tag{2}$$

III. RESULTS

A. Multiphoton tomography of human skin

The resolution of the tomograph was characterized first by determination of the PSF. Interestingly, we observed a laser beam induced displacement of nano- and microbeads when immersed in aqueous solution, similar to optical tweezers. Therefore, the PSF was determined on nanobeads in air (dried on a microscope slide). A lateral resolution of 0.4 μm [full width at half maximum (FWHM)] was determined, while the axial resolution reached 3 μm (FWHM). The measured maximum mean power after transmission of 88 mW corresponds to a transmittance of about 13%. The pulse width of the laser at the entrance of the system was 61 fs and was considerably stretched by the different optical elements to 310 fs. This resulted in a maximum output peak intensity of about 55 GW/cm^2 and pulse energy of about 0.1 nJ.

The imaging performance on biological tissue of the system with the gigahertz laser was tested with commonly used leaves of *Elodea densa* by generating multiphoton images to check the image quality prior to skin measurements. We were able to induce the multiphoton autofluorescence of the chloroplasts and cell structures (Fig. 3). Subsequent scans of the sample revealed no visible changes in the image, even with full laser power.

We performed tomography of the skin of a forearm. Images at different tissue depths z (with an increment of dz =5 μm) were recorded (Fig. 4). Compared to earlier results with megahertz laser systems, we observed the same features in the different layers of the skin at a similar image quality (contrast and SNR).[4] Starting at the surface in the stratum
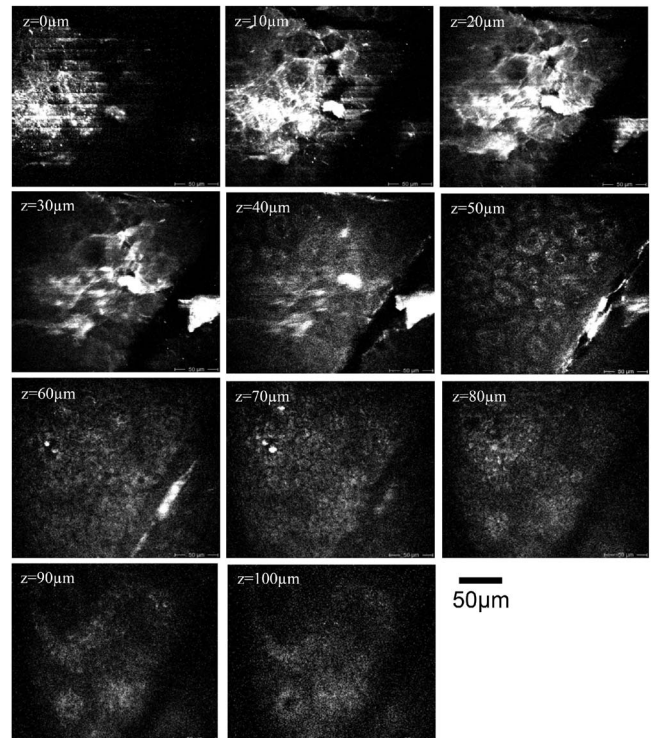

FIG. 4. High-resolution multiphoton autofluorescence tomography of human skin. Eleven optical sections from different tissue depths out of a stack are depicted.

corneum ($z=0-20$ μm) the typical hexagonal shaped cell structures of the stratum corneum ($z=10$ μm) were clearly identified. Regular horizontal line structures in the upper epidermis arise from motion artifacts, in particular, the volunteer's pulse beat. In deeper areas the living cells in the stratum spinosum (keratinocytes) are visible. With increasing imaging depth the cross section of the cells gets smaller until the stratum basale was reached. The junction epidermis/dermis indicated by the presence of papillae started at a typical value of about 80 μm. It was possible to obtain multiphoton autofluorescence images throughout the whole epidermal layer until an imaging depth of $z=100$ μm.

Figure 5 demonstrates a high-resolution autofluorescence image of the keratinocytes in the stratum spinosum showing the known composition of autofluorescence images of keratinocytes. In accordance with standard multiphoton imaging, the cell nuclei did not exhibit an autofluorescence signal in the visible spectral range.

B. Nanosurgery

On unlabeled specimens no chromosome dissection was achieved with the described configuration (gigahertz laser system with scanning microscope). Apparently the power density was insufficient to induce photodisruption. By staining with the chromophore blend Giemsa, the threshold for optical breakdown was significantly reduced. In this case we were able to process the chromosomes to realize incisions and to drill holes with dimensions in the submicron range.

Optical images of the chromosomes before and after laser irradiation are depicted in Fig. 6; the cutting lines are clearly visible. The effects of laser processing were analyzed
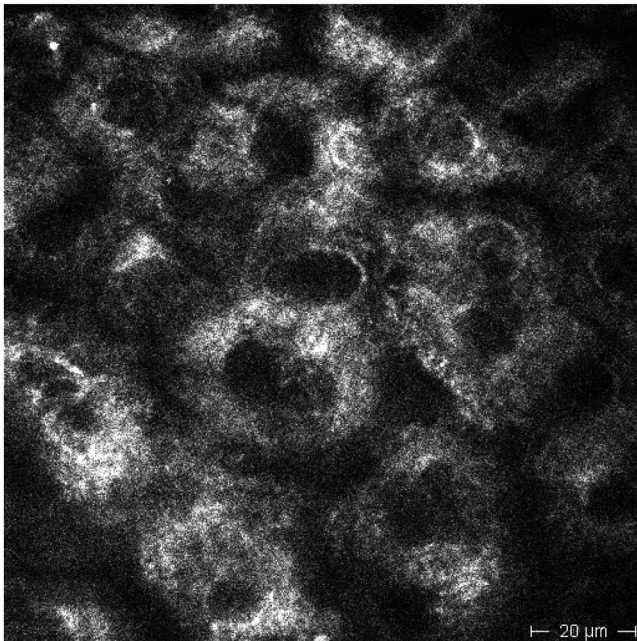
FIG. 5. Two-photon autofluorescence image of cells in the stratum spinosum at 40 μm depth. Single mitochondria can be resolved.

by measuring the surface morphology and size laser processed features with atomic force microscopy, see Fig. 7. The measurements revealed cut sizes ranging from 250 to 300 mm and holes with diameters of 700 nm.

IV. DISCUSSION

A preliminary test of the image performance was realized with a simple cell sample from plant tissue, *Elodea* leaves. A clear contrast in the range of 0.7–0.8 ($\pm$0.05) and a SNR of 10 ($\pm$0.5) show a good performance of the tested configuration. As mentioned, consecutive images of the sample configuration remained unaltered, thus showing no evidence of instantaneous degradation of the sample features.

In imaging human skin, we observed morphological structures of the different skin layers as already observed in experiments with megahertz laser sources by König and Riemann.[4] In accordance to these former examinations, the fluorescence signal arises from the same area in the different cell layers. Therefore, in the case of gigahertz lasers the major fluorescence component responsible for image formation found in the stratum corneum is keratin produced in the keratinocytes. In the stratum spinosum, the reduced coenzyme NAD(P)H mainly located in the organelles contributes the most to the autofluorescence signal. Single organelles in the cytoplasm of the cells were identified in accordance to the earlier experiments.

For quantitative analysis, the SNR and contrast were computed according to Eqs. (1) and (2) and compared to the above mentioned earlier studies with a megahertz laser source. In the stratum corneum, the SNR is in the range of 5–7 ($\pm$2) with a contrast of 0.6–0.7 ($\pm$0.05) for the system employing the gigahertz laser, while typical values with the megahertz systems are 5–8 ($\pm$2) and 0.6–0.7 ($\pm$0.05) for SNR and contrast, respectively. In the stratum spinosum, the SNR drops to 1.5–3 ($\pm$0.5) and the contrast to 0.12–0.3 ($\pm$0.03) with the gigahertz system, while typical values with the megahertz system are 2–3 ($\pm$0.5) and 0.1–0.4 ($\pm$0.05) for SNR and contrast, respectively.

In multiphoton microscopy and tomography, the conventionally used megahertz-Ti:sapphire lasers are driven at average powers of 10–40 mW, resulting in pulse energies of 0.2–0.5nJ.[4,20] In comparison with these standard systems, the gigahertz laser employed in this work had to be operated at an average power of 88 mW to obtain similar fluorescence intensities. With this unusual high laser powers we realized multiphoton fluorescence images with comparable SNR and contrast values. However, this rather high average power effectively resulted in pulse energies still one order of magnitude lower than for megahertz laser sources.

Typical relaxation times of the excited states of fluorescent molecules found in biological tissue are in the region of a few nanoseconds.[4] The time window between two subsequent laser pulses is 12.5 ns for a typical 80 MHz laser system, whereas it is only 1 ns for the 1 GHz system and therefore shorter or equal to the molecule relaxation times. Therefore, the probability of excited molecules absorbing energy from a subsequent laser pulse rises and excited state absorption is more likely to occur. The resulting energy buildup is likely to result in molecule ionization and molecule dissociation. However, unaltered images were obtained in consecutive scans of the same areas, thus revealing no instantaneous visible degradation.

In contrast, destructive effects can be induced under especially prepared conditions, in particular, in stained biological samples where the threshold for optical breakdown is reduced. We demonstrated multiphoton ablation effects in Giemsa stained human chromosomes by single point illumination and line scanning. In earlier works[10] König *et al.* reported an ablation threshold of about 1.6 TW/cm^2 for the nanodissection of unlabeled chromosomes using a Ti:sapphire laser source with a pulse duration of 170 fs, a repetition rate of 80 MHz, and an average power of 40 mW, resulting in a pulse energy of about 0.5 nJ. For Giemsa-labeled chromosomes the ablation threshold was reduced by a factor of 2.7. The maximum power density obtained with the gigahertz oscillator is about 55 GW/cm^2 with the galvoscanning microscope and therefore not sufficient to process unlabeled chromosomes.
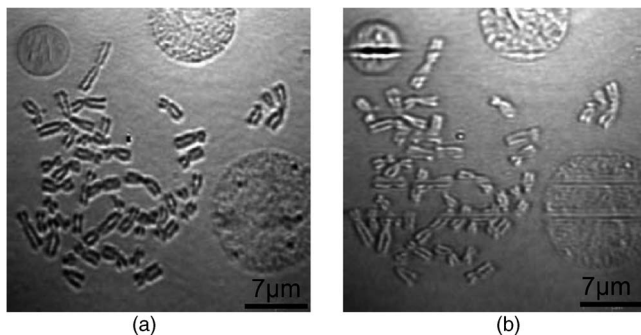

(a)   (b)

FIG. 6. Laser cutting effects in Giemsa labeled human chromosomes and intact interphase blood cells (a) before laser processing and (b) after laser irradiation
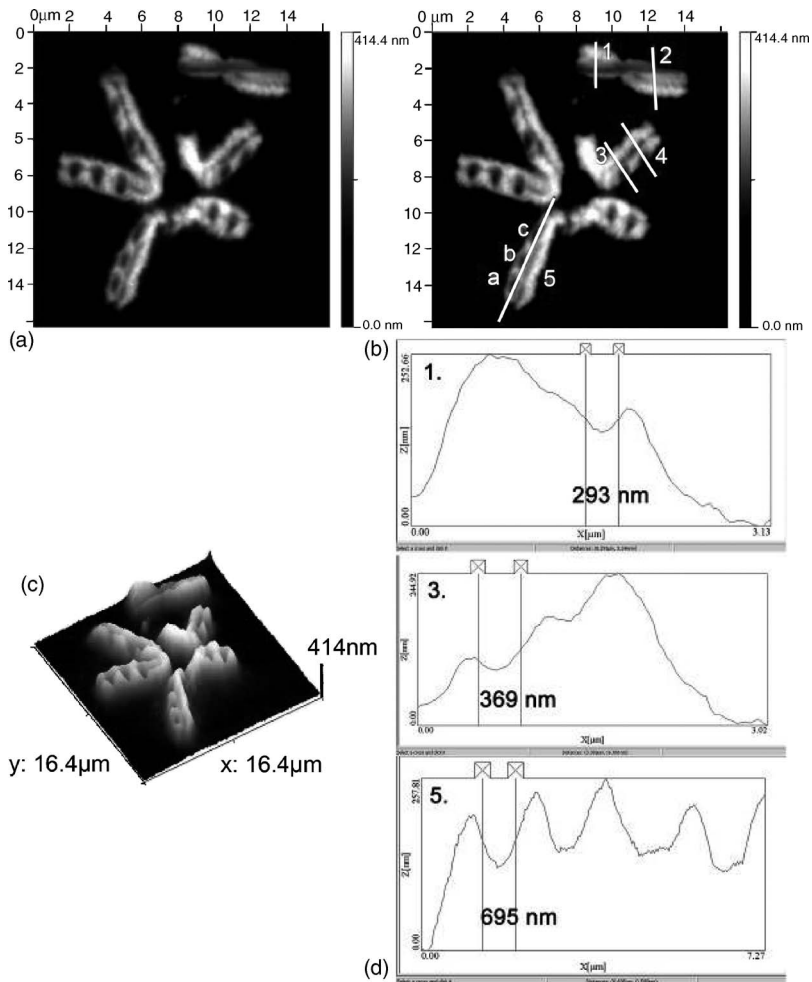
FIG. 7. (a) Nanodissection and nanodrilling of labeled human chromosomes. An atomic force microscope (AFM) has been employed to measure the nanprocessing dimensions. (b) The lines indicate where the cuts and holes were measured. (c) Three-dimensional (3D) profile. (d) Examples of surface profiles of cuts and holes.

By labeling the chromosomes, the ionization threshold of the targets is reduced so that the effect of excited state absorption is supposed to be able to generate the required energies for cutting or drilling of the chromosome material. On the one hand, this shows that the gigahertz laser can be used for the nanodissection of chromosomes and potentially other biological materials. On the other hand, it emphasizes the observations made with gigahertz multiphoton microscopy that the damage potential of on single pulse as well as the train of pulses with short temporal distance is not sufficient to induce damage to the specimen under examination. Rather, the consecutive pulses add to compensate the single pulse energies and add up to produce proper image qualities.

V. CONCLUSIONS

It was shown that gigahertz laser sources can successfully be used in multiphoton microscopy and nanomedicine. The achieved image quality was as good as that obtained with standard megahertz laser sources and produced the same features. Nanodissection could be demonstrated only on stained chromosomes. Since the time window between two pulses is in the range of the autofluorescence decay lifetimes of the target molecules, different physical effects compared to standard megahertz multiphoton microscopy have to be considered. Gigahertz femtosecond oscillators have the potential to become interesting multiphoton tools for high-

resolution diagnostics and nanoprocessing of a variety of materials. Further systems have to be optimized regarding transmission and pulse broadening to be able to increase the transient laser intensities at the target of interest. As the development of beam scanners and photomultipliers advances to faster systems, gigahertz laser systems offer the additional advantage of an increased number of pulses during the pixel dwell time. This results in an increased fluorescence of a certain pixel in the obtained image.

[1]B. R. Masters, P. T. So, and E. Gratton, Biophys. J. **72**, 2405 (1997).
[2]B. R. Masters, P. T. So, and E. Gratton, Ann. N.Y. Acad. Sci. **838**, 58 (1998).
[3]R. F. Hendriks and G. W. Lucassen, Proc. SPIE **4164**, 116 (2000).
[4]K. König and I. Riemann, J. Biomed. Opt. **8**, 432 (2003).
[5]T. Richter *et al.*, Skin Pharmacol. Appl. Skin Physiol. **17**, 246 (2004).
[6]K. König, A. Ehlers, F. Stracke, and I. Riemann, Skin Pharmacol. Appl. Skin Physiol. **19**, 78 (2006).
[7]M. J. Koehler, K. König, P. Elsner, R. Bückle, and M. Kaatz, Opt. Lett. **31**, 2879 (2006).
[8]S.-W. Chu, T.-M. Liu, C.-K. Sun, C.-Y. Lin, and H.-J. Tsai, Opt. Express **11**, 933 (2003).
[9]K. König, O. Krauss, and I. Riemann, Opt. Express **10**, 171 (2002).
[10]K. König, I. Riemann, P. Fischer, and K. J. Halbhuber, Cell Mol. Biol. (Paris) **45**, 195 (1999).
[11]K. König, I. Riemann, and W. Fritzsche, Opt. Lett. **26**, 819 (2001).
[12]K. König, I. Riemann, F. Stracke, and R. Le Harzic, Med. Laser Appl. **20**, 169 (2005).
[13]I. Maxwell, S. Chung, and E. Mazur, Med. Laser Appl. **20**, 193 (2005).
[14]A. Vogel, J. Noack, G. Hüttman, and G. Paltauf, Appl. Phys. B: Photophys. Laser Chem. **81**, 1015 (2005).

[15] A. Bartels, T. Dekorsy, and H. Kurz, Opt. Lett. **24**, 996 (1999).

[16] A. Bartels, T. Dekorsy, and H. Kurz, Conference on Lasers and Electro-Optics 2001, OSA Technical Digest Series, 2001, pp. 27–28.

[17] W. R. Zipfel, R. M. Williams, and W. W. Webb, Nat. Biotechnol. **21**, 1369 (2003).

[18] A. Babu and R. Verma, *Human Chromosomes: Principles & Techniques*, 2nd ed. (McGraw-Hill, New York, 1995).

[19] P. Lichter, A. L. Boyle, T. Cremer, and D. C. Ward, Genet. Anal.: Tech. Appl. **8**, 24 (1991).

[20] F. Fischer, B. Volkmer, S. Puschmann, R. Greinert, W. Breitbart, J. Kiefer, and R. Wepf, Proc. SPIE **6191**, 619105 (2006).